Predictive painting across faults

Zhiguang Xue[1], Xinming Wu[1], and Sergey Fomel[1]

Abstract

Predictive painting can effectively spread information in 3D volumes following the local structures (dips) of seismic events. However, it has trouble spreading information across faults with significant displacement. To address this problem, we incorporate fault-slip information into predictive painting to correctly spread information across faults. The fault slip is obtained using a local similarity scan to measure local shifts of the different sides of a fault. We have developed three methods to use the fault-slip information: (1) the area partition method, which uses the fault slip to correct the painting result after predictive painting in each divided area; (2) the fault-zone replacement method, which replaces fault zones with smooth transitions calculated with the fault slip information to avoid sharp jumps; and (3) the unfaulting method, in which we use the fault slip information to unfault the volume, perform predictive painting in the unfaulted domain, and then map the painting result back to the original space. Our methods are tested in application of predictive painting to horizon picking. Numerical examples demonstrate that predictive painting after incorporating fault slip information can correctly spread information across faults, which makes the proposed three approaches of using fault-slip information effective and applicable.

Introduction

Spreading some specific information following the local structures accurately and efficiently is important in many geophysical applications, such as seismic flattening (Lomask, 2003; Parks, 2010; Wu and Hale, 2015a, 2015b) and horizon picking in seismic interpretation, structure-oriented interpolation (Swindeman and Fomel, 2015), smoothing, and denoising. The predictive painting method, proposed by Fomel (2010), is a numerical algorithm that can spread information from a seed trace to its neighbors recursively following local dips with superior computational performance. Predictive painting has been used in different applications. For example, Fomel (2010) uses it to flatten seismic common-midpoint (CMP) gathers and to pick horizons in 3D image volumes; Liu et al. (2010) apply it to generate an extended dimension of seismic images to realize structure-oriented smoothing operator for removing nonconforming noise; Casasanta and Fomel (2011) use it for the CMP τ-p moveout correction and for the estimation of interval vertical transverse isotropy parameters; and Karimi and Fomel (2015), Zhang and Fomel (2016), and Shi et al. (2017) use it for image-guided well-log interpolation.

All these applications are based on the assumption that the local dip estimation required by predictive painting is correct. However, when the spreading space contains faults, accurate dip estimation can be challenging due to the existence of conflicting dips. Even when the estimated dip on both sides of the fault is correct, it may not characterize the correct displacement across the fault. We propose to incorporate fault slip information to predictive painting to make it spread information across faults correctly. Fault slip can be estimated by correlating seismic reflectors on the opposite sides of a fault. Aurnhammer and Tonnies (2005) and Liang et al. (2010) propose windowed crosscorrelation methods. Hale (2013) and Wu et al. (2016) use a dynamic warping method that obviates correlation windows. In this paper, the fault slip is estimated using a local similarity scan (Fomel, 2007a; Fomel and Jin, 2009). The local similarity scan method can estimate a relative time (or depth) shift map between two images, which is similar to that of the dynamic warping method, and it is more accurate than that of the windowed crosscorrelation method when local shifts vary rapidly (Hale, 2013). Compared with dynamic warping, the local similarity scan has the advantage of using normalized amplitudes and picking a regularized path with subpixel accuracy.

We propose three methods of using the fault slip information in predictive painting: area partition, fault-

[1]The University of Texas at Austin, Bureau of Economic Geology, John A. and Katherine G. Jackson School of Geosciences, Austin, Texas, USA. E-mail: zhiguangxue@utexas.edu; xinming.wu@beg.utexas.edu; sergey.fomel@beg.utexas.edu.

Manuscript received by the Editor 18 September 2017; revised manuscript received 12 December 2017; published ahead of production 16 February 2018; published online 06 April 2018. This paper appears in *Interpretation*, Vol. 6, No. 2 (May 2018); p. T449–T455, 4 FIGS.

http://dx.doi.org/10.1190/INT-2017-0171.1.

zone replacement, and unfaulting methods. The general idea of unfaulting is not new (Wei and Maset, 2005; Luo and Hale, 2013; Wu et al., 2016). We implement unfaulting of the seismic image by solving a regularized inverse problem using shaping regularization, which can help us to get the desired result faster (Fomel, 2007b). In the following, we first briefly review the theory of predictive painting and describe the proposed methods. Then, we apply predictive painting to horizon picking, and we use several 2D benchmark examples to test the performance of these methods.

Theory

Brief review of predictive painting

Predictive painting spreads information from a seed trace to its neighbors recursively by following the local dip (Fomel, 2010). The spreading or "painting" process can be implemented using a plane-wave construction filter (Fomel and Guitton, 2006). The mathematical basis of this filter is a differential equation for local plane waves (Claerbout, 1992),

$$\frac{\partial P}{\partial x}+\sigma\frac{\partial P}{\partial t}=0, \tag{1}$$

where $P(t,x)$ is the wavefield and σ is the local slope. In the case of a constant slope, equation 1 has the simple general solution

$$P(t,x)=f(t-\sigma x), \tag{2}$$

where $f(t)$ is an arbitrary waveform. Equation 2 is nothing more than a mathematical description of a plane wave. Assuming that the slope $\sigma(t,x)$ varies in time and space, we can design a local operator to propagate trace $\mathbf{s}_i$ to trace $\mathbf{s}_j$, and we describe such prediction as $\mathbf{A}_{i,j}$. If $\mathbf{s}_r$ is a reference trace, spreading its information to a distant neighbor $\mathbf{s}_k$ (e.g., $k>r$) can be accomplished by the simple recursion

$$\mathbf{s}_k=\mathbf{A}_{k-1,k}\cdots\mathbf{A}_{r+1,r+2}\mathbf{A}_{r,r+1}\mathbf{s}_r. \tag{3}$$

The recursive operator in equation 3 is referred to as *predictive painting* (Fomel, 2010).

Application limitation with faults

The accuracy of predictive painting depends on the accuracy of dip estimation (Fomel, 2002). However, the local dip attribute may not characterize the fault displacement correctly. For example, Figure 1a shows a synthetic 2D image that contains a fault with a constant slope 1, but the local fault slip is nonstationary, changing from −10 to 10 samples. To estimate the local fault slip, we extract the traces on the opposite sides of the fault (as indicated by the dashed lines in Figure 1a) and use a local similarity scan (Fomel, 2007a) to measure the local shifts. A local similarity scan involves two steps: scanning and picking. Figure 1b shows the similarity scan, and the black curve on it represents the picked local fault throw, which is the vertical component of the fault slip. The curve is picked by regarding the local similarity as a velocity field and then solving the eikonal equation twice with a source on the top and bottom boundaries, respectively (Fomel, 2009). The picked local fault slip matches the theoretical value (a sine function), and we can use it in the application of predictive painting.

Methods

Next, we describe three methods of incorporating fault slip information into predictive painting for crossing through faults accurately.

Area partition method

This method consists of three steps:

1) Divide original volume into $n+1$ small volumes based on fault surfaces assuming that the fault number is n.
2) Pad all the small volumes with zero slope (horizontally) to make them only contain complete traces.
3) Do the following iterations: Perform predictive painting in the first small volume, then use the fault slip information of the first fault to correct the painting result, and repeat these two steps until the predictive painting is complete in the last small volume.

The area partition method is based on two observations: (1) Predictive painting treats a whole trace as the basic unit, and (2) predictive painting with a zero slope does not change the spreading information. This method adopts the divide-and-conquer strategy and it depends on the explicit area partition, so it is simple

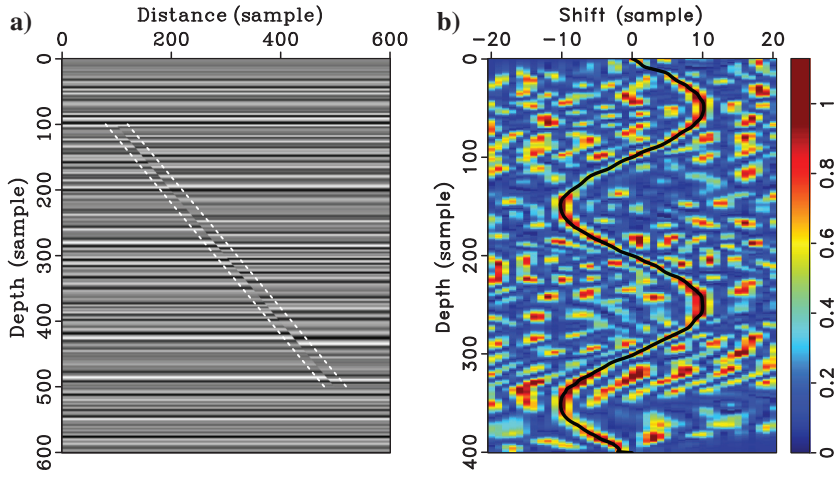

Figure 1. (a) A 2D synthetic image containing a fault that has a constant slope of 1 but nonstationary fault slips and (b) a fault throw (the vertical component of slip) measured using the local similarity scan.

to implement as long as the original image is easily divisible.

Fault-zone replacement method

To remove the effect of faults, we can also replace fault zones with smooth transitions, and then the original image becomes an image without faults. The smooth transition is designed with the fault slip information, and the width of the fault zone can be chosen based on the magnitude of the fault slip. When the fault slip is large, it is easier to avoid aliasing in the smooth transition zone by selecting a wider fault zone.

If the width of a fault zone is N samples, we can extract two traces at $-N/2$ samples (left side) and $N/2$ samples (right side) of the fault, and then we do linear interpolation to generate the traces from $-N/2+1$ to $N/2-1$ as the transition zone. Note that the linear interpolation cannot be done horizontally if the fault slip is not zero. It has to be along the slip vector direction. A simple way to follow such a direction is to do linear interpolation through predictive painting and set the dip to be the fault throw (the vertical component of slip) divided by $N-1$. Specifically, the fault transition would be the distance-weighted sum of the predictive painting results of the two selected traces. This method is also simple to implement, but if the faults are close to each other, an appropriate fault-zone width may be hard to choose.

Unfaulting method

Similar to fault-zone replacement, we can also undo faulting in a seismic image to align seismic reflectors across faults. Following the theory part of the unfaulting method in Wu et al. (2016), we solve a similar regularized linear equation to get the shift vector $\mathbf{s}(\mathbf{x})$ where $\mathbf{s} \equiv (s_1, s_2, s_3)$ and coordinates $\mathbf{x} \equiv (x_1, x_2, x_3)$ (1, 2, and 3 are the indices representing different spatial dimensions). Shift vector $\mathbf{s}(\mathbf{x})$ means that we can unfault the image if the sample at $\mathbf{x}$ moves to $\mathbf{x}+\mathbf{s}(\mathbf{x})$.

If $\mathbf{x}_a$ is a left point of a fault, we can use local similarity to estimate its fault slip vector $\mathbf{t}(\mathbf{x}_a)$, which can provide us with a simple linear equation:

$$\mathbf{s}(\mathbf{x}_a + \mathbf{t}(\mathbf{x}_a)) - \mathbf{s}(\mathbf{x}_a) = \mathbf{t}(\mathbf{x}_a). \tag{4}$$

This linear equation only applies to those samples alongside faults. For other samples away from faults, we expect unfaulting shifts to vary slowly and continuously along structural directions. This constraint can be added to the inverse problem by using a gradient operator as a regularization term (Wu et al., 2016) or by using a structure-oriented smoothing operator as a

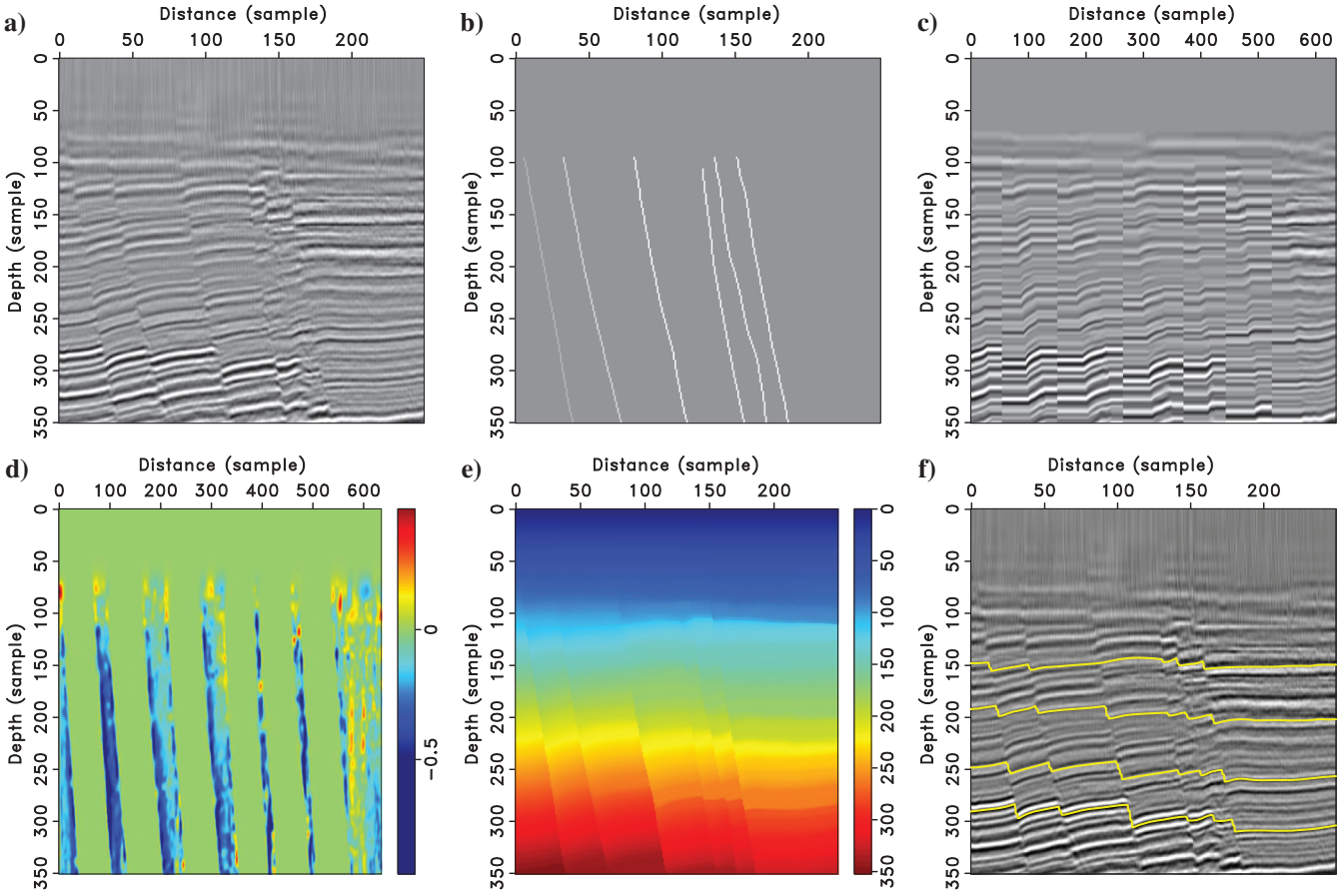

Figure 2. A 2D example for the area partition method. (a) Original image, (b) fault mask, (c) new image after area partition and padding with zero slope, (d) dip of the new image (dip around the vertical boundaries is set to be zero), (e) final predictive painting result (displayed on the original grid mesh), and (f) several automatically picked horizons.

shaping operator in the framework of shaping regularization (Fomel, 2007b). We choose the latter, and solve for the shift vector $\mathbf{s}(\mathbf{x})$ using the method previously used by Xue et al. (2016).

After we get the shift vector $\mathbf{s}(\mathbf{x})$, we unfault the original image $f(\mathbf{x})$ to a fault-free image $\tilde{f}(\mathbf{x})$ by doing an inverse interpolation:

$$\tilde{f}(\mathbf{x}+\mathbf{s}(\mathbf{x}))=f(\mathbf{x}). \tag{5}$$

Then, we can estimate dip from the new image and perform predictive painting to get a painting result $\tilde{p}(\mathbf{x})$, which can be converted to the painting result $p(\mathbf{x})$ of the original image $f(\mathbf{x})$ by doing a forward interpolation:

$$p(\mathbf{x})=\tilde{p}(\mathbf{x}+\mathbf{s}(\mathbf{x})). \tag{6}$$

Examples

In this section, we use three 2D examples to verify the effectiveness of the proposed three methods. We test an application of predictive painting for horizon picking on all of the 2D images. In this application, the depth coordinate is regarded as the reference trace being spread recursively from left to right. The spreading result is referred to as relative geologic time (Stark, 2004), and each contour of it represents a horizon. All of the images contain several faults, and we want to correctly pick several horizons using our methods of predictive painting across faults. The fault maps in all the examples are estimated using the method proposed by Wu and Hale (2016).

Example for area partition method

Figure 2 shows the example for the area partition method. A 2D poststack seismic image from a historic Gulf of Mexico data set (Claerbout, 2006) is shown in Figure 2a. As shown by the fault mask (Figure 2b), the image contains six faults. We extract the left and right traces of the six faults, and we use the local similarity scan to estimate their fault slips. Then based on the six faults, we divide the image into seven small parts and pad all the small parts horizontally to make each of them a rectangle. The new combined image is shown in Figure 2c. It has a larger horizontal dimension and contains six vertical boundaries that are the locations where we would serially correct the results of predictive painting in the small padded areas. Figure 2d shows the dip estimated from the new image, and the dip around the boundaries has been set to be zero. With this dip, we perform predictive painting and simultaneously correct the painting result at each

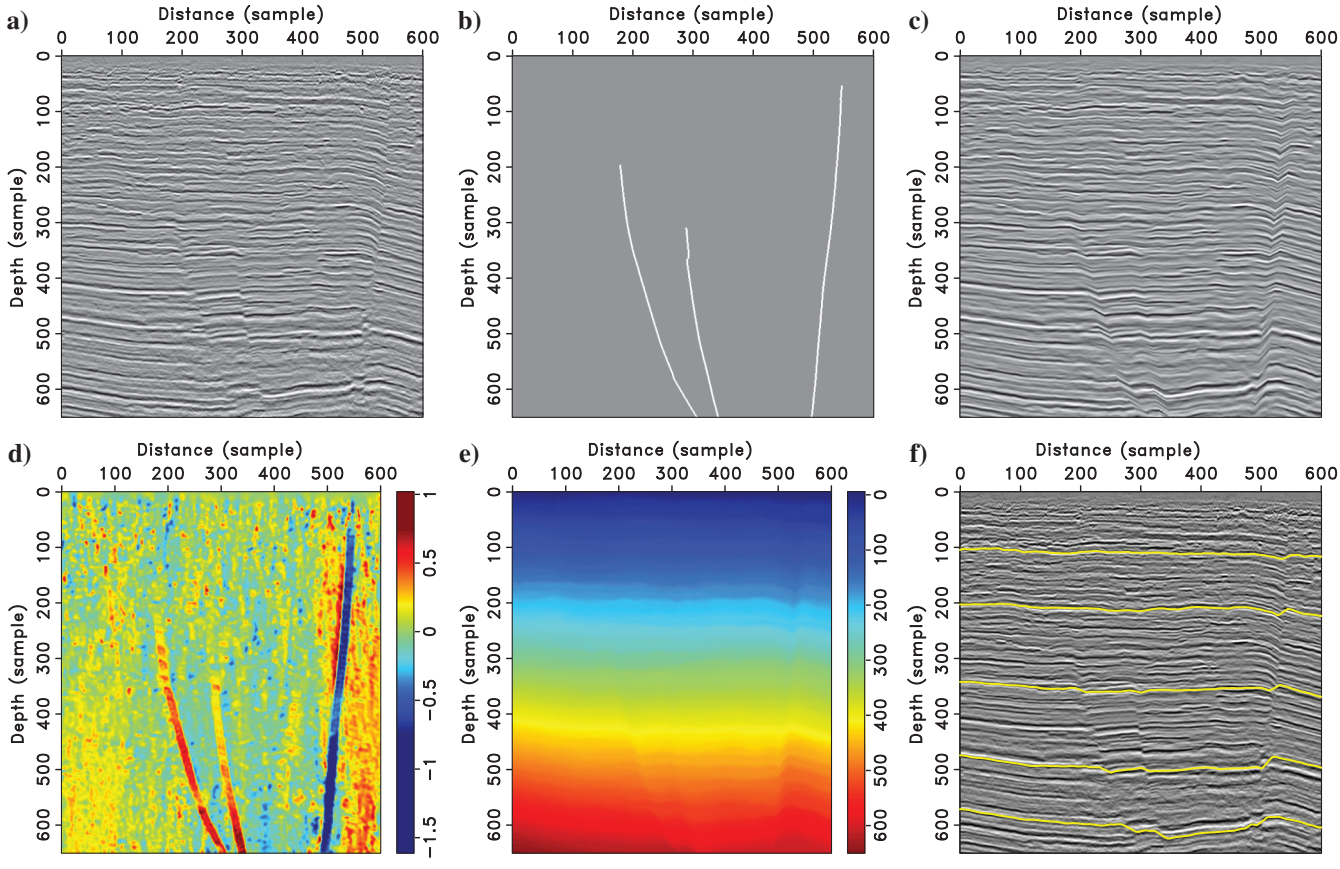

Figure 3. A 2D example for the fault-zone replacement method. (a) Original image, (b) fault mask, (c) new image after replacing the fault zones with smooth transitions, (d) dip of the new image, (e) predictive painting using dip in Figure 3d, and (f) several automatically picked horizons.

boundary. The predictive painting result only corresponding to the original image is recorded, which is shown in Figure 2e, in which we can observe abrupt value changes alongside the faults. The picked horizons as indicated by the yellow lines in Figure 2f follow the true horizons accurately.

Example for fault-zone replacement method

Figure 3 shows the example for the fault-zone replacement method, and it has the same layout as Figure 2. Figure 3a shows the original image and it contains three faults (Figure 3b). Because the fault slip of the three faults is not very large, we set the fault zone width to be 17 samples for all the faults. The new image after the fault-zone replacement with smooth transitions is shown in Figure 3c, and the two sides of the faults have been smoothly bridged. The dip of the new image is shown in Figure 3d, from which we can easily detect the fault zones: three narrow bands. Figure 3e shows the predictive painting result and it contains smoothly varying bands instead of sharp cliffs, which are also implied by the yellow curves in Figure 3f. When the hori-

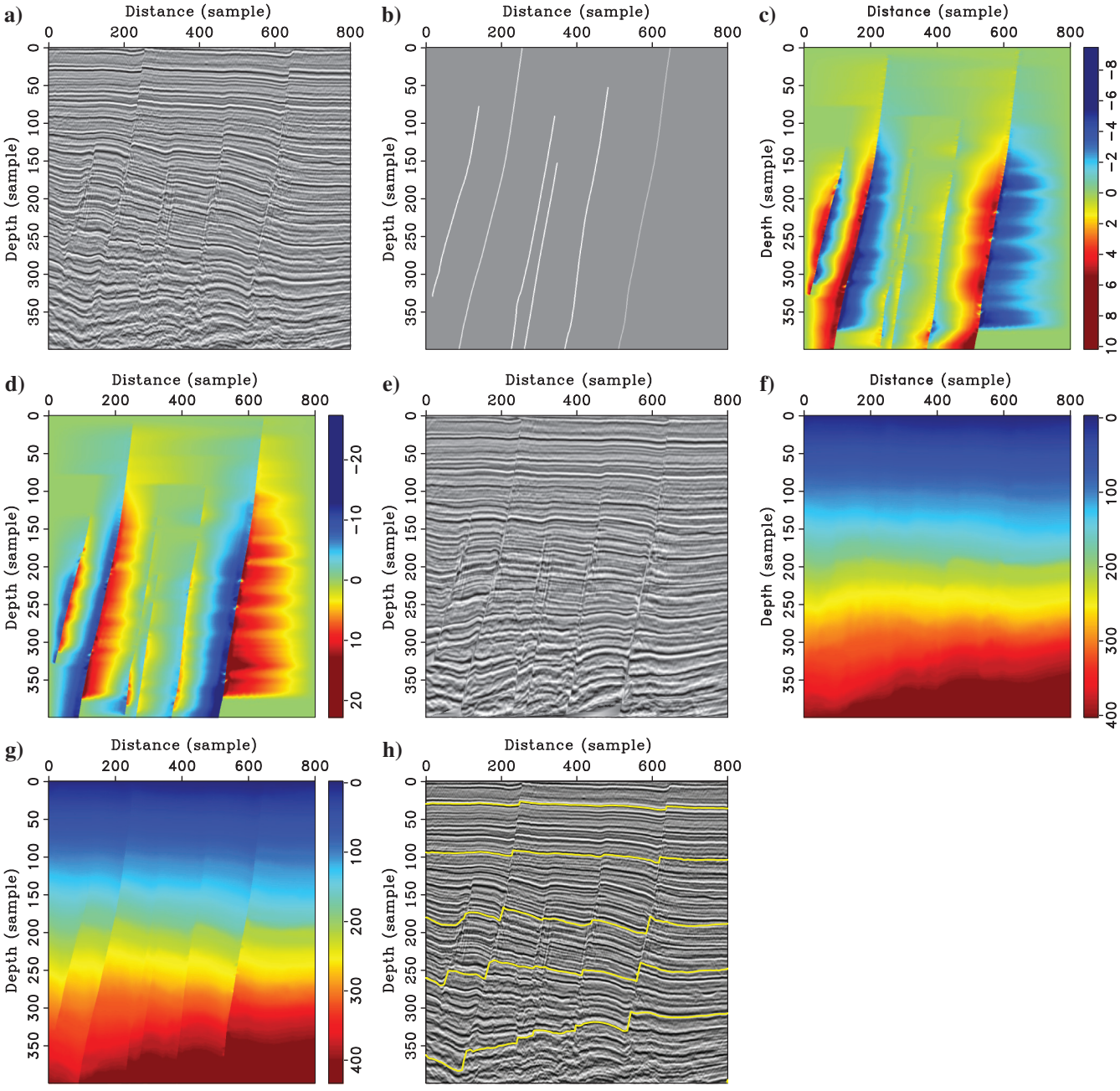

Figure 4. A 2D example for the unfaulting method. (a) Original image, (b) fault mask, (c) the horizontal component of the shift vector, (d) the vertical component of the shift vector, (e) new image after undoing the faulting of the original image, (f) predictive painting of the unfaulted image, (g) predictive painting of the original image, obtained by faulting the result in Figure 4f, and (h) several automatically picked horizons.

zon curves cross through the faults, they jump slowly from one side to the other side.

Example for unfaulting method

Figure 4 shows the example for the unfaulting method. The image (Figure 4a) contains six faults, and the fault slip of the second and last faults is relatively large. We first solve a regularized inverse problem based on equation 4 using shaping regularization to obtain the shift vector (Figure 4c and 4d), and then we unfault the original image to an image shown in Figure 4e. After unfaulting, the seismic events have been aligned across the faults. Then, we estimate dip from the new image and carry out predictive painting to get the result shown in Figure 4f. To get the predictive painting result of the original image, we interpolate the result in Figure 4f back to the original coordinates, and we get the result in Figure 4g, in which the sharp changes caused by fault displacements can be clearly observed. Figure 4h shows several picked horizons overlaid on the original image. The consistency between the yellow curves and the true horizons verifies the effectiveness of the unfaulting method.

Conclusion

We propose to incorporate fault slip information into predictive painting to help it spread information across the faults correctly. Three methods of processing the fault slip information have been presented, and numerical tests have verified their effectiveness. We use the application of automatic horizon picking to test the proposed methods in the examples. The area partition and the fault-zone replacement methods are efficient and easy to implement. However, the former requires dividing the 2D section or 3D volume into small parts, which may be challenging for complicated fault structures, and the latter requires us to select an appropriate fault zone width to avoid aliasing issues, which may be difficult for images with dense fault distributions. In these two cases, we suggest using the more powerful unfaulting method. The unfaulting method can work well in complex faulting scenarios, such as horsts and grabens. When unfaulting the image with intersecting faults, it is necessary to move fault blocks and faults themselves. Compared with the first two methods, the unfaulting method has a much higher computational cost. A 3D extension of the three methods is straightforward once the fault curves are replaced by fault hypersurfaces.

Acknowledgments

We thank the associate editor G. Dutta and three anonymous reviewers for providing valuable suggestions. We also thank the sponsors of the Texas Consortium for Computational Seismology for financial support. The first author was additionally supported by the Statoil Fellows Program at the University of Texas at Austin. All computations presented in this paper are reproducible using the Madagascar software package (Fomel et al., 2013).

References

Aurnhammer, M., and K. Tonnies, 2005, A genetic algorithm for automated horizon correlation across faults in seismic images: IEEE Transactions on Evolutionary Computation, **9**, 201–210, doi: 10.1109/TEVC.2004.841307.

Casasanta, L., and S. Fomel, 2011, Velocity-independent F020τ–p moveout in a horizontally layered VTI medium: Geophysics, **76**, no. 4, U45–U57, doi: 10.1190/1.3595776.

Claerbout, J. F., 1992, Earth soundings analysis: Processing versus inversion: Blackwell Scientific Publications.

Claerbout, J. F., 2006, Basic earth imaging: Stanford Exploration Project.

Fomel, S., 2002, Applications of plane-wave destruction filters: Geophysics, **67**, 1946–1960, doi: 10.1190/1.1527095.

Fomel, S., 2007a, Local seismic attributes: Geophysics, **72**, no. 6, A29–A33, doi: 10.1190/1.2437573.

Fomel, S., 2007b, Shaping regularization in geophysical-estimation problems: Geophysics, **72**, no. 2, R29–R36, doi: 10.1190/1.2433716.

Fomel, S., 2009, Velocity analysis using AB semblance: Geophysical Prospecting, **57**, 311–321, doi: 10.1111/j.1365-2478.2008.00741.x.

Fomel, S., 2010, Predictive painting of 3-D seismic volumes: Geophysics, **75**, no. 4, A25–A30, doi: 10.1190/1.3453847.

Fomel, S., and A. Guitton, 2006, Regularizing seismic inverse problems by model reparameterization using plane-wave destruction: Geophysics, **71**, no. 5, A43–A47, doi: 10.1190/1.2335609.

Fomel, S., and L. Jin, 2009, Time-lapse image registration using the local similarity attribute: Geophysics, **74**, no. 2, A7–A11, doi: 10.1190/1.3054136.

Fomel, S., P. Sava, I. Vlad, Y. Liu, and V. Bashkardin, 2013, Madagascar: Open-source software project for multidimensional data analysis and reproducible computational experiments: Journal of Open Research Software, **1**, e8, doi: 10.5334/jors.ag.

Hale, D., 2013, Methods to compute fault images, extract fault surfaces, and estimate fault throws from 3D seismic images: Geophysics, **78**, no. 2, O33–O43, doi: 10.1190/geo2012-0331.1.

Karimi, P., and S. Fomel, 2015, Image guided well log interpolation using predictive painting: 85th Annual International Meeting, SEG, Expanded Abstracts, 2786–2790.

Liang, L., D. Hale, and M. Maučec, 2010, Estimating fault displacements in seismic images: 80th Annual International Meeting, SEG, Expanded Abstracts, 1357–1361.

Liu, Y., S. Fomel, and G. Liu, 2010, Nonlinear structure-enhancing filtering using plane-wave prediction: Geophysical Prospecting, **58**, 415–427, doi: 10.1111/(ISSN)1365-2478.

Lomask, J., 2003, Flattening 3D seismic cubes without picking: 73rd Annual International Meeting, SEG, Expanded Abstracts, 1402–1405.

Luo, S., and D. Hale, 2013, Unfaulting and unfolding 3D seismic images: Geophysics, **78**, no. 4, O45–O56, doi: 10.1190/geo2012-0350.1.

Parks, D., 2010, Seismic image flattening as a linear inverse problem: M.S. thesis, Colorado School of Mines.

Shi, Y., X. Wu, and S. Fomel, 2017, Well-log interpolation guided by geologic distance: 87th Annual International Meeting, SEG, Expanded Abstracts, 1939–1944.

Stark, T., 2004, Relative geologic time (age) volume: Relating every seismic sample to a geologically reasonable horizon: The Leading Edge, **23**, 928–932, doi: 10.1190/1.1803505.

Swindeman, R., and S. Fomel, 2015, Seismic data interpolation using plane-wave shaping regularization: 85th Annual International Meeting, SEG, Expanded Abstracts, 3853–3858.

Wei, K., and R. Maset, 2005, Fast faulting reversal — Draft version 3: 75th Annual International Meeting, SEG, Expanded Abstracts, 771–774.

Wu, X., and D. Hale, 2015a, 3D seismic image processing for unconformities: Geophysics, **80**, no. 2, IM35–IM44, doi: 10.1190/geo2014-0323.1.

Wu, X., and D. Hale, 2015b, Horizon volumes with interpreted constraints: Geophysics, **80**, no. 2, IM21–IM33, doi: 10.1190/geo2014-0212.1.

Wu, X., and D. Hale, 2016, 3D seismic image processing for faults: Geophysics, **81**, no. 2, IM1–IM11, doi: 10.1190/geo2015-0380.1.

Wu, X., S. Luo, and D. Hale, 2016, Moving faults while unfaulting 3D seismic images: Geophysics, **81**, no. 2, IM25–IM33, doi: 10.1190/geo2015-0381.1.

Xue, Z., Y. Chen, S. Fomel, and J. Sun, 2016, Seismic imaging of incomplete data and simultaneous-source data using least-squares reverse-time migration with shaping regularization: Geophysics, **81**, no. 1, S11–S20, doi: 10.1190/geo2014-0524.1.

Zhang, R., and S. Fomel, 2016, Application of predictive painting to well-log data interpolation and seismic inversion: 86th Annual International Meeting, SEG, Expanded Abstracts, 3582–3586.

Biographies and photographs of the authors are not available.